Spin Crossover

DOI: 10.1002/ange.200601823

A Manganese(III) Complex That Exhibits Spin Crossover Triggered by Geometric Tuning**

Grace G. Morgan, Kevin D. Murnaghan, Helge Müller-Bunz, Vickie McKee, and Charles J. Harding*

Dedicated to Professor Jane Nelson

The design and synthesis of molecules with potential for information storage and processing is a focus in current materials research, an area in which bulk metal oxides still predominate. The potential of discrete transition-metal spin-crossover (SCO) complexes in this area is now starting to be realized as photoinduced switching emerges as an increasingly efficient trigger for spin conversion.[1] As the field continues to grow, it is important to identify new candidates with improved thermal or optical responses and also to fine-tune the molecular design for successful incorporation into devices.

Although the phenomenon is theoretically possible for octahedral d^{4-7} ions, it is routinely observed only in Fe^{II} and Fe^{III} complexes, and to a lesser extent in Co^{II} complexes. This situation highlights the delicate balance between ligand-field strength, ionic charge, and the number of d electrons in determining SCO activity. For example, the contrast between the spin-labile Fe^{II} center and its d^6 analogue Co^{III} lies in the higher nuclear charge of Co^{III}, which stabilizes the $S=0$ state. Similarly, SCO is rarely observed in Mn^{II} (d^5) complexes, in which the high-spin (HS) state is usually stabilized, in contrast to the isoelectronic Fe^{III} ion, for which many examples of spin conversion exist.[2]

Spin transitions in d^4 ions are, however, the most rare. The two potential candidates are Mn^{III} and Cr^{II} and although thermal SCO has been reported for both ions[3,4] it is considered exceptional. The best-known example is [Mn(trp)] (trp^{3-} = tris{1-(2-azolyl)-2-azabuten-4-yl}amine),[3] and investigations of its physical properties continue.[5,6] The only other well-characterized example $[CrI_2(depe)_2]$[4] (depe = 1,2-bis-(diethylphosphino)ethane) also continues to attract attention.[7] An early report of some Mn^{III} complexes, which were not structurally characterized, attributes the temperature dependence of the magnetic moment to exchange interactions, although SCO is a more likely interpretation.[8]

An important driving force for SCO is the change in metal–ligand bond length arising from the increased vibrational entropy in the HS state. The concomitant decrease in ligand-field splitting energy reduces the ligand-field stabilization energy (LFSE) associated with the maximum population of the t_{2g} orbitals. The reluctance of octahedral d^4 ions to undergo thermal SCO may be due to the very minor gain in LFSE on crossover from ^5E to ^3T as only one electron is transferred. In most crystal fields, the small LFSE gain for d^4 ions is outweighed by the energetic penalty of pairing two electrons, which results in both an increase in the destabilizing Coulomb repulsion energy π_c and a decrease in the stabilizing exchange energy π_e.[9]

Schiff base ligands with $N_4(O^-)_2$, $N_2(O^-)_2$, and $N_3(O^-)_3$ donor sets that are known to generate ligand fields close to the crossover value for Fe^{III}[10] tend to stabilize manganese in its +III oxidation state, in which it is normally HS. Recently, however, we have observed that modulation of the orientation of the $N_4(O^-)_2$ donors in a series of hexadentate ligands has a dramatic effect on the spin state of Mn^{III} complexes and that gradual thermal SCO may be attained when the phenolate oxygen donors are *trans* to each other. This geometry is achieved by varying the length of the alkyl chains in the starting tetraamine. The use of a triethylenetetraamine link (in L1) orients the oxygen donors *cis* to each other and produces a HS Mn^{III} complex, whereas lengthening the link by two methylene groups (L2) orients the oxygen donors in *trans* geometry and thermal SCO results.

To illustrate this phenomenon, we report the structures and temperature dependence of the magnetic susceptibility of $[MnL1]NO_3\cdot EtOH$ (**1**) and $[MnL2]NO_3$ (**2**), which exhibit different geometries of the $N_4(O^-)_2$ donor set. The syntheses of the perchlorate salts of both complexes have been reported as part of an investigation into their electron-transfer activity.[11]

L1 forms a temperature-independent HS complex with Mn^{III} (**1**), which has a magnetic moment of 4.8 μ_B between 80 and 300 K. In contrast, the magnetic moment of complex **2** has significant temperature dependence (Figure 1). The absence of a plausible pathway for intermolecular exchange

---

[*] Dr. G. G. Morgan, Dr. K. D. Murnaghan, Dr. H. Müller-Bunz
Centre for Synthesis and Chemical Biology
Conway Institute for Biomedical and Biomolecular Research and
School of Chemistry and Chemical Biology
University College Dublin
Belfield, Dublin 4 (Ireland)
Fax: (+353) 1-716-2127
E-mail: grace.morgan@ucd.ie

Prof. V. McKee
Department of Chemistry
Loughborough University
Leicestershire, LE11 3TU (UK)

Dr. C. J. Harding
Department of Chemistry
The Open University
Walton Hall, Milton Keynes, MK7 6AA (UK)

[**] The authors would like to thank the University College Dublin, Enterprise Ireland, and the Royal Society of New Zealand (ISAT Linkages Fund) for financial support and the University of Otago for hosting a sabbatical visit (to G.G.M.) during manuscript preparation.

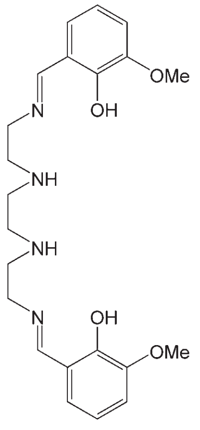

H_2L1

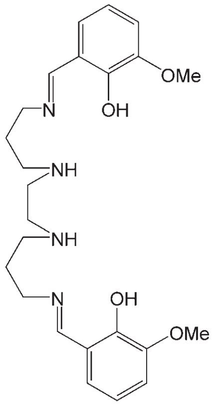

H_2L2

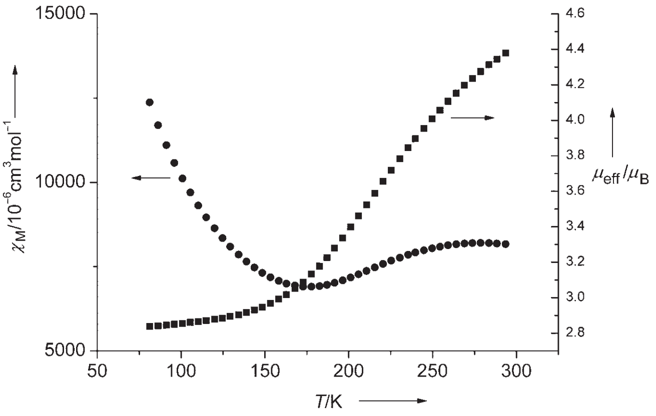

Figure 1. χ_M and μ_{eff} versus *T* for **2**.

and the sigmoid form of this temperature dependence confirms this process as SCO. At 80 K, the magnetic moment converges close to the expected LS value of 2.8 μ_B whereas at 300 K the HS limit is entropically inaccessible, as this is a one-electron SCO.[12] The gradual nature of the crossover reflects the inefficient communication between discrete Mn^{III} sites which is mediated only by weak hydrogen bonding.

Crystallographic data for **1** were collected at 100 K and for **2** at 100 and 300 K;[13] selected bond lengths for all structural determinations are given in Table 1, and structures of **1** and **2** (100 K) are shown in Figure 2 with a comparison of the Mn coordination spheres in both complexes shown in Figure 3.

Table 1: Selected bond lengths [Å] for **1** at 100 K and for **2** at 100 K and 300 K and differences in bond lengths for **2** between 100 K and 300 K (Δr_{HL}).

	1	**2**	**2**	**2**
	100 K	100 K	300 K	Δr_{HL}
$Mn{-}N_{imine}$	1.992(2) 2.051(2)	1.9883(11)	2.0723(19)	0.0840
$Mn{-}N_{amine}$	2.064(2) 2.301(2)	2.0501(11)	2.161(2)	0.1109
Mn−O	2.0889(18) 1.8873(18)	1.8719(9)	1.8679(13)	−0.0040

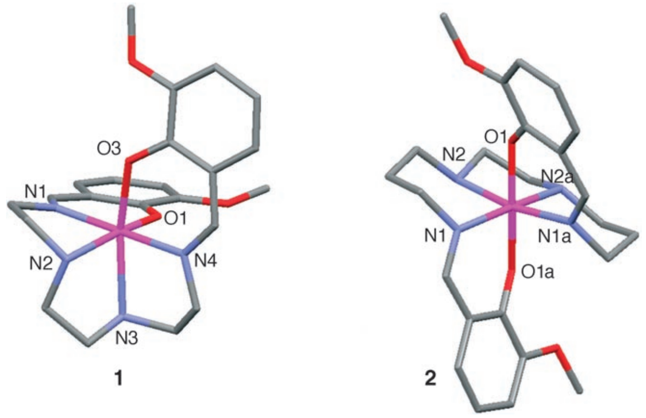

Figure 2. Structures of **1** and **2** at 100 K ($a = 0.5-x$, $0.5-y$, z).

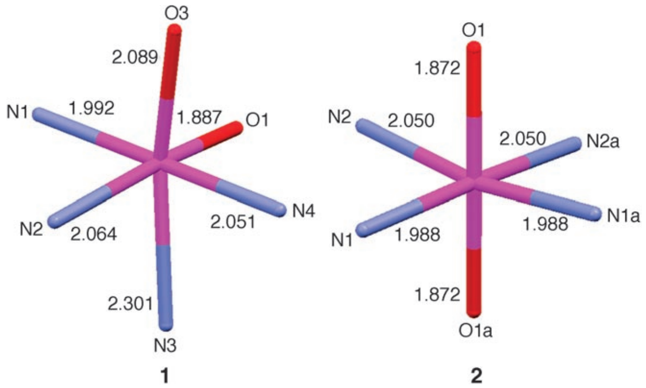

Figure 3. Comparison of Mn–donor bond lengths in **1** and **2** at 100 K ($a = 0.5-x$, $0.5-y$, z).

HS octahedral complexes of d^4 transition-metal ions are expected to display larger radii, and hence longer metal–ligand bonds, than their LS counterparts. Additionally, distortions due to Jahn–Teller splitting are expected for the ^5E state. In the HS complex **1**, the geometry around Mn is distorted octahedral with two *cis* oxygen donors (O1 and O3), two *cis* amines (N2 and N3), and two *trans* imine nitrogen donors (N1 and N4). The long bonds to one of the oxygen atoms (O3) and one of the amine nitrogen atoms (N3) are in accordance with the expected static axial elongation. Structural data for the SCO complex **2** at both collection temperatures show that the geometry around Mn is again pseudooctahedral but now with the two oxygen donors oriented *trans* to each other and with more regular geometry. A twofold rotation axis through the Mn center bisects the ethylene linkage between the two amine nitrogen atoms N2 and N2a to generate geometrically equivalent pairs of *cis* imine (N1 and N1a), *cis* amine (N2 and N2a), and *trans* phenolate (O1 and O1a) donors.

Comparison of the bond lengths in **1** and **2** at 100 K (Figure 3) reveals a significant increase in the average Mn–donor bond lengths in the HS complex **1** over those in the LS

SCO complex **2**, and the significant change in the sum of the bond lengths (12.384 Å for **1** compared with 11.821 Å for **2**) is consistent with different orbital populations for the two complexes at 100 K.

Of greater significance is the comparison between the bond lengths of **2** at the two collection temperatures (Figure 4). The most striking feature is the significant elongation of all four equatorial Mn–N bond lengths in sharp contrast to the axial Mn–O bond lengths, which remain unchanged. This structural change is in good agreement with population of the antibonding $d_{x^2-y^2}$ orbital upon switching to the HS state (Figure 5), which should result in longer equatorial distances relative to the ^{3}T state.

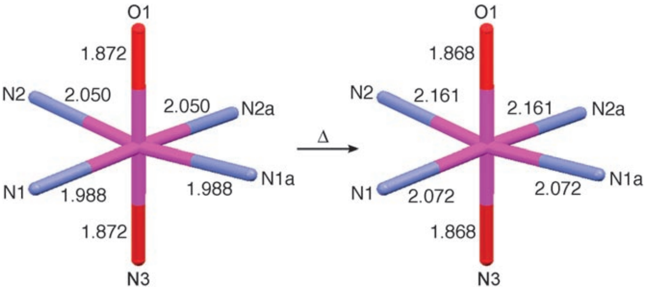

Figure 4. Comparison of Mn–donor distances in **2** at 100 K and 300 K ($a = 0.5-x$, $0.5-y$, z).

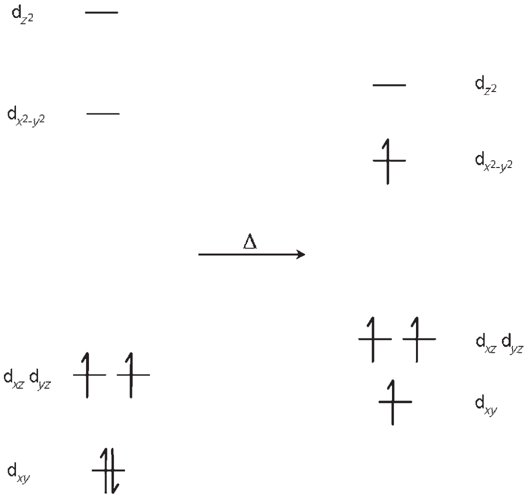

Figure 5. Orbital populations for the $S = 1$ and $S = 2$ states of **2**.

Thermal population of the $d_{x^2-y^2}$ orbital rather than the d_{z^2} orbital as a result of the SCO produces an unusual axial compression in the predominantly HS form of **2** at 300 K. Axially compression in HS Mn^{III} complexes is rare and is often associated with significant geometric distortion, which is not observed here.[14]

The bond length difference between the high- and low-spin ions (Δr_{HL}) is not expected to be as large for d^4 metals as it is for ions with d^5 and d^6 configurations, as only one electron is removed from an antibonding orbital upon transition to the $S = 1$ state in d^4 complexes. In Fe^{II} complexes, the bond-length change may be as large as 0.2 Å, whereas the smaller changes upon crossover in Fe^{III} complexes (typically ca. 0.1 Å) are ascribed to the asymmetric population of the t_{2g} orbital set in the LS state, in which one electron hole exists.[14]

The change in bond lengths for d^4 SCO complexes upon moving from $S = 2$ to $S = 1$ should therefore be expected to be significantly less than for d^5 complexes, as only one electron is removed from the e_g* orbital set and two electron holes remain in the t_{2g} orbitals upon switching to the ^{3}T state. The bond-length change in **2** is 0.06 Å (averaged over all six donors), which is in line with the expected trend.

The flexible open-chain chelating ligand L2 can readily accommodate the necessary structural changes that accompany SCO. This situation is more difficult to achieve with a macrocylic ligand such as cyclam (1,4,8,11-tetraazacyclotetradecane), which also coordinates Mn^{III} with an N$_4$ equatorial donor set, and with various exogenous axial donors.[15] When these are cyano ligands, the LS state of the Mn^{III} complex is stabilized with short axial bonds but surprisingly long equatorial bonds.[15b] Presumably the more rigid macrocycle constrains the contraction of the equatorial bonds that is expected in LS Mn^{III} complexes.

In conclusion, we have demonstrated that thermal SCO in Mn^{III} complexes is accessible with the $N_4(O^-)_2$ donor set of L2 and that the effect was triggered by orienting the methoxy-substituted phenolate donors *trans* to each other in the more flexible ligand. No crossover was observed when the phenolate donors were *cis*, and orientation of the donors, and thus the SCO phenomenon, was controlled by modification of the chain length of the chelating ligand. This result opens up a route to the synthesis of a new family of d^4 SCO candidates, and work is already underway to establish the series.

Experimental Section

1: 3-Methoxy-2-hydroxy-benzaldehyde (0.92 g, 6 mmol) in ethanol (30 mL) was added to triethylenetetraamine (0.73 g, 3 mmol) in ethanol (15 mL), and then solid $Mn(NO_3)_2 \cdot 6H_2O$ (0.54 g, 3 mmol) was added. Dark-brown crystals precipitated from the filtered solution after 48 h. Yield: 220 mg (13.5 %). Elemental analysis (%) calcd for $C_{24}H_{34}N_5O_8Mn$: C 50.09, H 5.95, N 12.17; found: C 49.72, H 5.91, N 12.09.

2: Neat *N,N'*-Bis(3-aminopropyl)ethylenediamine (0.54 g, 3.1 mmol) was added to a solution of 3-methoxy-2-hydroxy-benzaldehyde (0.99 g, 6.5 mmol) in ethanol (25 mL), and then solid $Mn(NO_3)_2 \cdot 6H_2O$ (0.54 g, 3 mmol) was added. The solution was heated to reflux for 20 minutes and filtered while hot. Black crystals formed almost instantly on cooling. Yield: 650 mg (39 %). Elemental analysis (%) calcd for $C_{24}H_{32}N_5O_7Mn$: C 51.71, H 5.79, N 12.56; found: C 51.67, H 5.75, N 12.52.

Magnetic susceptibilities were measured between 80 and 300 K on a Faraday balance calibrated with $Hg[Co(NCS)_4]$. Experimental susceptibilities were corrected for the diamagnetism of the constituent atoms by using Pascal's constants. Crystal data for **1** and **2** were collected at 100 K on a Bruker SMART APEX CCD area detector diffractometer and for **2** at 300 K on a Bruker SMART 1000 diffractometer. Crystal-structure pictures were generated with Mercury.[16]

Received: May 9, 2006

Keywords: ligand design · magnetic properties · manganese · molecular switches · spin crossover

---

[1] a) A. Hauser, *Top. Curr. Chem.* **2004**, *234*, 155–198; b) S. Bonhommeau, G. Molnár, A. Galet, A. Zwick, J.-A. Real, J. J. McGarvey, A. Bousseksou, *Angew. Chem.* **2005**, *117*, 4137–4141; *Angew. Chem. Int. Ed.* **2005**, *44*, 4069–4073.

[2] P. J. van Konigsbruggen, Y. Maeda, H. Oshio, *Top. Curr. Chem.* **2004**, *233*, 259–324.

[3] P. G. Sim, E. Sinn, *J. Am. Chem. Soc.* **1981**, *103*, 241–243.

[4] D. M. Halepoto, D. G. L. Holt, L. F. Larkworthy, G. L. Leigh, D. C. Povey, G .W. Smith, *J. Chem. Soc. Chem. Commun.* **1989**, 1322–1323.

[5] Y. Garcia, O Kahn, J-P. Ader, A. Buzdin, Y. Meurdesoif, M. Guillot, *Phys. Lett.* A **2000**, *271*, 145–154.

[6] a) M. Nakano, G. Matsubayashi, T. Matsuo, *Phys. Rev. B* **2002**, *66*, 212412–212415; b) S. Kimura, Y. Narumi, D. Kindo, M. Nakano and G. Matsubayashi, *Phys. Rev. B* **2005**, *72*, 064448.

[7] V. Ksenofontov, A. B. Gaspar, G. Levchenko, B. Fitzsimmons, P. Gütlich, *J. Phys. Chem.* B **2004**, *108*, 7723.

[8] V. V. Zelentsov, I. K. Somova, *Zh. Obshch. Khim.* **1974**, *44*, 1309–1313.

[9] Y. Garcia, P. Gütlich, *Top.Curr.Chem.* **2004**, *234*, 49–62.

[10] J.-P. Costes, F. Dahan, J.-P. Laurent, *Inorg. Chem.* **1990**, *29*, 2448–2452.

[11] a) A. Panja, N. Shaikh, R. J. Butcher, P. Banerjee, *Inorg. Chim. Acta* **2003**, *352*, 27–33; b) A. Panja, N. Shaikh, S. Gupta, R. J. Butcher, P. Banerjee, *Eur. J. Inorg. Chem.* **2003**, 1540–1547.

[12] P. Gütlich, Y. Garcia, H. Spiering, *Magnetism: Molecules to Materials*, *Vol. IV* (Ed.: J. S. Miller, M. Drillon), Wiley-VCH, Weinheim, **2002**, Chapter 8.

[13] Crystal data for **1** (at 100(2) K): $0.30\times0.05\times0.02$ mm^3, monoclinic, $P2_1/c$, $a=17.661(2)$, $b=11.836(1)$, $c=12.863(1)$ Å, $\beta=105.595(2)°$, $V=2589.8(5)$ Å^3, $\rho_{calcd}=1.476$ Mg m^{-3}, $2\theta_{max}=50.00°$, Mo$_{K\alpha}$ ($\lambda=0.71073$ Å), φ-ω-scans, 18064 reflections collected, 4548 unique (all included in refinement), correction for Lorentzian polarization and absorption: semi-empirical from equivalents (program SADABS,[17a] $\mu=0.568$ mm^{-1}, max. and min. transmission 0.9887 and 0.8583), solution: direct methods (SHELXS-97[17b]), refinement: full-matrix least-squares against $|F^2|$ (SHELXL-97-2[17c]), 346 parameters, hydrogen atoms were added at calculated positions and refined by using a riding model, $R_1=0.059$, $wR_2=0.099$, residual electron density: 0.431 e$^-$ Å^{-3}. Crystal data for **2** (at 100(2) K): $0.5\times0.4\times0.2$ mm^3, orthorhombic, $Pccn$, $a=17.837(1)$, $b=8.4113(6)$, $c=16.813(1)$ Å, $V=2589.8(5)$ Å^3, $\rho_{calcd}=1.468$ Mg m^{-3}, $2\theta_{max}=57.19°$, Mo$_{K\alpha}$ ($\lambda=0.71073$ Å), ϕ-ω-scans, 20136 reflections collected, 3078 independent (all included in refinement), correction for Lorentzian polarization and absorption: semi-empirical from equivalents (program SADABS,[17a] $\mu=0.577$ mm^{-1}, max. and min. transmission 0.8933 and 0.7764), solution: direct methods (SHELXS-97[17b]), refinement: full-matrix least-squares against $|F^2|$ (SHELXL-97-2[17c]), 233 parameters, hydrogen atoms were located in the difference Fourier map and allowed to refine freely, $R_1=0.034$, $wR_2=0.083$, residual electron density: 0.461 e$^-$ Å^{-3}. Crystal data for **2** (at 300(2) K): $0.65\times0.15\times0.10$ mm^3, orthorhombic, $Pccn$, $a=17.833(2)$, $b=8.914(1)$, $c=16.504(2)$ Å, $V=2623.8(6)$ Å^3, $\rho_{calcd}=1.411$ Mg m^{-3}, $2\theta_{max}=50.00°$, Mo$_{K\alpha}$ ($\lambda=0.71073$ Å), φ-ω-scans, 17576 reflections collected, 2314 independent (all included in refinement), correction for Lorentzian polarization and absorption: semi-empirical from equivalents (programs SADABS,[16d] SMART,[16e] and SAINT,[16e] $\mu=0.555$ mm^{-1}, max. and min. transmission 1.0000 and 0.8363). The structure was solved by direct methods and refined by full-matrix least-squares on F^2 by using the SHELXTL suite of programs.[16f] 172 parameters, hydrogen atoms bonded to carbon were added at calculated positions and refined by using a riding model. The hydrogen atom bonded to N2 was located from a difference map and refined with a fixed, isotropic displacement parameter. $R_1=0.048$, $wR_2=0.089$, residual electron density: 0.185 e$^-$ Å^{-3}. CCDC-605565 (**1** at 100 K), -605564 (**2** at 100 K), and -605566 (**2** at 300 K) contain the supplementary crystallographic data for this paper. These data can be obtained free of charge from The Cambridge Crystallographic Data Centre via www.ccdc.cam.ac.uk/data_request/cif.

[14] a) C. Mantel, A. K. Hassan, J. Pécaut, A. Deronzier, M.-N. Collomb, C. Duboc-Toia, *J. Am. Chem. Soc.* **2003**, *125*, 12337–12344; b) A. K. Gregson, D. M. Doddrell, P. C. Healy, *Inorg. Chem.* **1978**, *17*, 1216–1219.

[15] a) S. Mossin, H. Osholm Sørensen, H. Weihe, J. Glerup, I. Sotofte, *Inorg. Chim. Acta* **2005**, *358*, 1096–1106; b) S. Mossin, H. Osholm Sørensen, H. Weihe, *Acta Crystallogr. Sect. C* **2002**, *58*, m204–m206.

[16] I. J. Bruno, J. C. Cole, P. R. Edgington, M. K. Kessler, C. F. Macrae, P. McCabe, J. Pearson, R. Taylor, *Acta Crystallogr. Sect. B* **2002**, *58*, 389–397.

[17] a) G. M. Sheldrick, SADABS, Bruker AXS Inc., Madison, WI 53711, USA, **2000**; b) G. M. Sheldrick, SHELXS-97, University of Göttingen, **1997**; c) G. M. Sheldrick SHELXL-97-2, University of Göttingen, **1997**; d) G. M. Sheldrick, SADABS, Bruker AXS Inc., Madison, WI 53711, USA, **2003**; e) Bruker **1998** SMART (version 5.625 and SAINT (version 6.02), Bruker AXS, Madison, WI 53711, USA; f) G. M. Sheldrick, SHELXTL version 6.12, **2001**, Bruker AXS, Madison, WI 53711, USA.